

# Optical properties of erbium-doped organic polydentate cage complexes

L. H. Slooff<sup>a)</sup> and A. Polman

*FOM Institute for Atomic and Molecular Physics, Kruislaan 407, 1098 SJ Amsterdam, The Netherlands*

M. P. Oude Wolbers, F. C. J. M. van Veggel, and D. N. Reinhoudt

*Supramolecular Chemistry and Technology, University of Twente, P.O. Box 217, 7500 AE Enschede, The Netherlands*

J. W. Hofstraat

*Akzo Nobel Central Research, Department RGL, P.O. Box 9300, 6800 SB Arnhem, The Netherlands*

(Received 7 July 1997; accepted for publication 16 September 1997)

The optical properties of different erbium (Er)-doped polydentate hemispherand organic cage complexes are studied, for use in polymer-based planar optical amplifiers. Room temperature photoluminescence at 1.54  $\mu\text{m}$  is observed, due to an intra- $4f$  transition in  $\text{Er}^{3+}$ . The Er is directly excited into one of the  $4f$  manifolds (at 488 nm), or indirectly (at 287 nm) via the aromatic part of the cage. The luminescence spectrum is 70 nm wide (full width at half maximum), the highest known for any Er-doped material, enabling high gain bandwidth for optical amplification. The absorption cross section at 1.54  $\mu\text{m}$  is  $1.1 \times 10^{-20} \text{ cm}^2$ , higher than in most other Er-doped materials, which allows the attainment of high gain. Measurements were performed on complexes in KBr tablets, in which the complex is present in the form of small crystallites, or dissolved in the organic solvents dimethylformamide and butanol-OD. In KBr the luminescence lifetime at 1.54  $\mu\text{m}$  is  $< 0.5 \mu\text{s}$ , possibly due to concentration quenching effects. In butanol-OD solution, the lifetime is 0.8  $\mu\text{s}$ , still well below the radiative lifetime of 4 ms estimated from the measured absorption cross sections. Experiments on the selective deuteration of the near-neighbor C–H bonds around the  $\text{Er}^{3+}$ -ion indicate that these are not the major quenching sites of the  $\text{Er}^{3+}$  luminescence. Temperature dependent luminescence measurements indicate that temperature quenching is very small. It is therefore concluded that an alternative luminescence quenching mechanism takes place, presumably due to the presence of O–H groups on the Er-doped complex (originating either from the synthesis or from the solution). Finally a calculation is made of the gain performance of a planar polymer waveguide amplifier based on these Er complexes, resulting in a threshold pump power of 1.4 mW and a typical gain of 1.7 dB/cm. © 1998 American Institute of Physics. [S0021-8979(97)06124-0]

## I. INTRODUCTION

Erbium (Er) doped materials have attracted a lot of attention, because of their potential applications in optoelectronics.<sup>1–3</sup> In its trivalent state the  $\text{Er}^{3+}$  ion shows an intra  $4f$  shell transition from its first excited state ( $^4I_{13/2}$ ) to the ground state ( $^4I_{15/2}$ ), which occurs at a wavelength of 1.54  $\mu\text{m}$ . In the free  $\text{Er}^{3+}$ -ion optical intra  $4f$  shell transitions are parity forbidden. Incorporated in a solid host however, the crystal field of the host induces mixing of states, which makes some of the transitions allowed. These optical transitions are rather sharp, due to the fact that the partially filled  $4f$  shell is shielded by filled  $5s$  and  $5p$  shells. The luminescence lifetime of the first excited state can be as long as several milliseconds.<sup>4–6</sup> These features make Er-doped materials very attractive for lasers and optical amplifiers operating at 1.54  $\mu\text{m}$ , one of the standard telecommunication wavelengths.

Er-doped planar optical amplifiers have been demonstrated using silica,<sup>7–12</sup>  $\text{Al}_2\text{O}_3$ ,<sup>13</sup> and  $\text{LiNbO}_3$ <sup>14,15</sup> hosts. However, as polymer waveguides are becoming more important, both as fibers and in thin film configurations, it is interesting to study the doping of planar polymer waveguides

with Er, and to investigate if optical amplification can be achieved. Such polymer amplifiers could then be integrated in existing optical polymer devices such as splitters, switches, and multiplexers<sup>16</sup> with low coupling losses.

The inorganic Er salts cannot be dispersed directly into an organic matrix. To avoid this problem, the  $\text{Er}^{3+}$ -ion must first be encapsulated by an organic ligand. The resulting complex can then be dispersed in a polymer film. The ligand has to be designed such that it provides enough coordination sites to bind the  $\text{Er}^{3+}$ -ion and to form a stable complex. Furthermore it may serve to shield the  $\text{Er}^{3+}$ -ion from impurities in the surrounding matrix that may quench the luminescence. For example, O–H is known to quench the luminescence due to coupling of the excited state of the ion to vibrational modes of the O–H bond.<sup>17–19</sup>

In this article we study the optical properties of different Er-doped polydentate hemispherands, which form an overall neutral complex in which the  $\text{Er}^{3+}$ -ion is encapsulated in a cagelike ligand configuration. Clear room temperature photoluminescence at 1.54  $\mu\text{m}$  is observed for these complexes with a luminescence lifetime up to 0.8  $\mu\text{s}$ . Selective deuteration experiments are carried out to study the possible quenching effect of C–H bonds. Exchanging C–H for C–D has been shown beneficial for  $\text{Eu}^{3+}$ .<sup>20</sup>

<sup>a)</sup>Electronic mail: Slooff@amolf.nl; <http://www.amolf.nl>

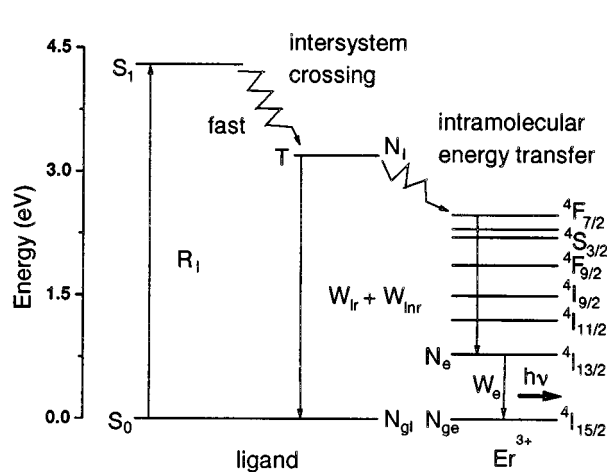


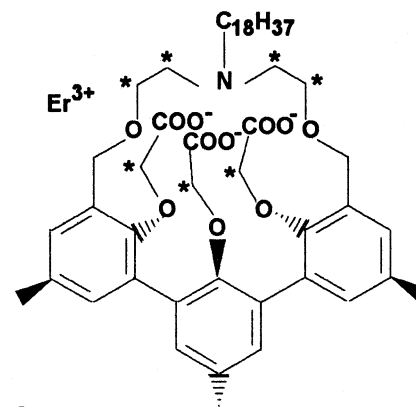
FIG. 1. Schematic diagram of the ligand-Er system. The complex is first excited from the singlet  $S_0$  ground state to the singlet  $S_1$  excited state (exact position not known, but higher lying than 3.2 eV), followed by fast relaxation to the triplet  $T$  state. From there, energy transfer to the  $\text{Er}^{3+}$  4f levels may take place. From these levels, rapid relaxation to the  $^4I_{13/2}$  first excited state in  $\text{Er}^{3+}$  takes place. Finally the  $\text{Er}^{3+}$  may decay to the  $^4I_{15/2}$  ground manifold by the emission of a  $1.54 \mu\text{m}$  photon. The various symbols in the figure are discussed in the text.

Two different types of excitation are studied: direct excitation in one of the  $\text{Er}^{3+}$  manifolds using a 488 nm Ar laser, and excitation via the organic ligand using a 337 nm  $\text{N}_2$  laser, followed by energy transfer to the  $\text{Er}^{3+}$  ion (see Fig. 1). The luminescence temperature quenching and the absorption spectral cross sections are discussed, and finally a performance estimate for a planar optical amplifier based on these Er-doped complexes is made.

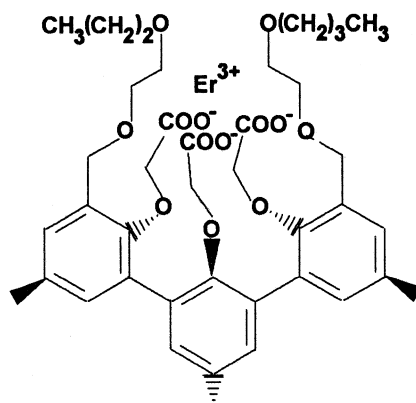
## II. EXPERIMENT

Three different  $\text{Er}^{3+}$ -complexes were prepared in a multistep synthesis, as discussed in detail in Ref. 20, and characterized by fast atom bombardment mass spectrometry, infrared spectroscopy, and elemental analysis. Figure 2(a) shows a schematic picture of a cyclic  $\text{Er}^{3+}$ -complex in which the first coordination sphere consists of either C-H bonds (cyc-H), or C-D bonds (cyc-D). An acyclic  $\text{Er}^{3+}$ -complex (acyc-H), sketched in Fig. 2(b), was also studied: it is open at the top and contains two  $\text{O}(\text{CH}_2)_3\text{CH}_3$  groups. This is slightly different compared to the cyclic complexes which are closed at the top and with one  $\text{C}_{18}\text{H}_{37}$  chain attached to the trivalent nitrogen atom. A three-dimensional representation of the cyclic complex is shown in Fig. 2(c).

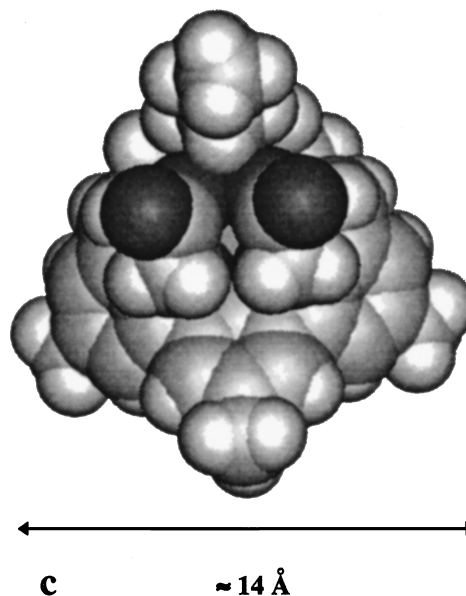
After synthesis, the  $\text{Er}^{3+}$ -complex solutions were dried, mixed with KBr and then pressed to 1 mm thick tablets with a diameter of 1.2 cm. The Er concentration is 1.0 wt. %. This concentration does not take into account the (unknown) amount of water which may remain in the tablets as a result of the preparation process. To exclude the effect of quenching due to O-H in the host, some measurements were performed on solutions in deuterated butanol ( $>98\%$ ) at a complex concentration of  $10^{-4}$  M or dimethylformamide (DMF) at a concentration of  $2 \times 10^{-3}$  M. In all solvents acyc-H dis-



a



b



c

FIG. 2. Two-dimensional representation of the structure of (a) the cyclic  $\text{Er}^{3+}$ -complex: \* represents either two H (cyc-H) or two D (cyc-D) atoms, and (b) the acyclic  $\text{Er}^{3+}$ -complex (acyc-H). The outer two benzene rings lie in one plane which is tilted backwards, whereas the middle benzene ring is tilted forwards. In this way a cage is constructed encapsulating the  $\text{Er}^{3+}$  ion. (c) Three-dimensional representation of the cyclic complex (cyc-H).

solved rather well, but the solutions with the cyclic complexes appeared somewhat turbid, indicating that not all the material had dissolved.

Photoluminescence (PL) measurements were performed using the 488 nm line of an Ar ion pump laser at a power of

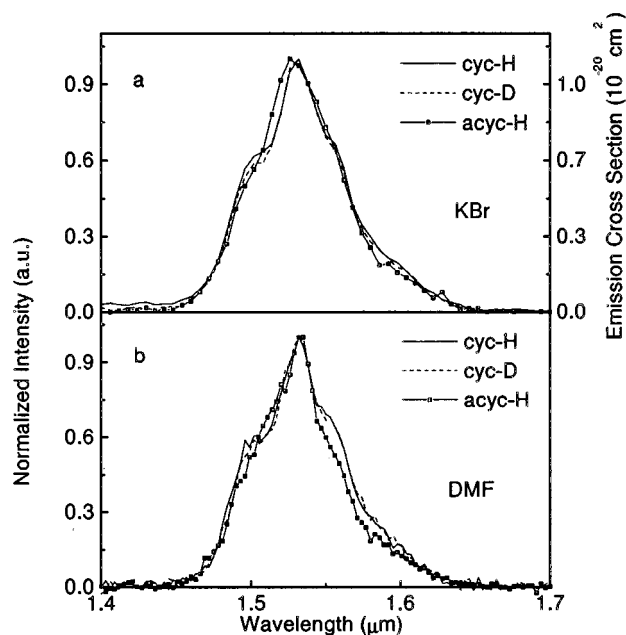


FIG. 3. Normalized room temperature PL spectra of  $\text{Er}^{3+}$ -complexes in (a) KBr tablets and (b) DMF, at a pump wavelength of 488 nm (power 100 mW).

100 mW for excitation. The laser beam was modulated with a mechanical chopper or an acousto-optic modulator at frequencies of 20 and 40 Hz. For the temperature dependent measurements, the samples were mounted in a closed-cycle helium cryostat, enabling measurements at temperatures ranging from 15 K to room temperature. The KBr tablets were first mounted onto a piece of crystalline silicon. The PL signal was focused into a monochromator and detected with a liquid-nitrogen-cooled Ge detector, using standard lock-in techniques. The spectral resolution was 6 nm. Luminescence lifetime measurements were performed by monitoring the luminescence decay after excitation with a 0.5 ns pulse of a  $\text{N}_2$  laser ( $\lambda_{\text{exc}} = 337$  nm, pulse energy 20  $\mu\text{J}$ , 10 Hz repetition rate). Decay signals were recorded using a cooled Ge detector with a time resolution of 0.3  $\mu\text{s}$ . The signals were averaged using a digitising oscilloscope. All decay curves were analysed by deconvolution of the measured detector response.

Reflection  $R$  and transmission  $T$  measurements were performed using a spectrometer measuring the reflected and transmitted intensities with an integrating sphere. The spectral resolution was 0.3 nm.

### III. RESULTS AND DISCUSSION

Figure 3(a) shows normalized room temperature PL spectra for the three complexes in KBr after excitation at 488 nm into the  $^4\text{F}_{7/2}$  level (see Fig. 1). The peak around 1.54  $\mu\text{m}$  is typical for  $\text{Er}^{3+}$  luminescence and is due to the transition from the first excited state ( $^4\text{I}_{13/2}$ ) to the ground state ( $^4\text{I}_{15/2}$ ). The full width at half maximum (FWHM) of all spectra is 70 nm. To our knowledge this is much wider than for any other Er-doped material: Er-implanted  $\text{SiO}_2$  (11 nm FWHM),<sup>21</sup> phosphosilicate glass (25 nm FWHM),<sup>21</sup> sodalime silicate

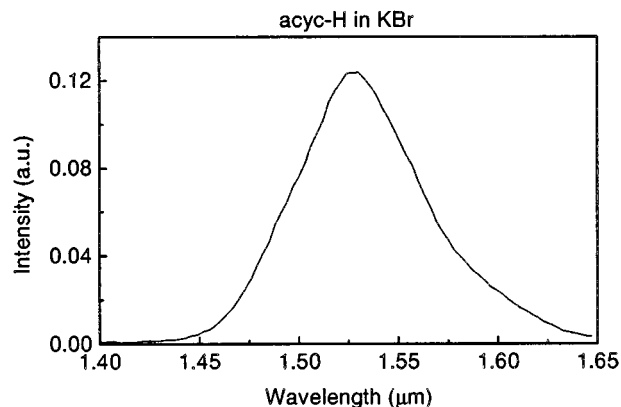


FIG. 4. Room temperature PL spectrum of acyc-H in KBr after excitation via the ligand at 337 nm (pulse energy 20  $\mu\text{J}$ ).

glass (19 nm FWHM),<sup>5</sup>  $\text{Al}_2\text{O}_3$  (55 nm FWHM),<sup>6</sup> and fluoro-hafnate glass (FWHM 64 nm).<sup>22</sup> Such a broad spectrum enables a wide gain bandwidth for optical amplification.

No comparison of the absolute PL intensities could be made for the three complexes, as the intensity varies over the KBr tablets (a factor 2–3). The spectral shapes measured for the two cyclic complexes are identical, and slightly different from that for the acyclic complex. This difference is attributed to a small difference in local environment for the two types of complexes. Figure 3(b) shows the normalized room temperature PL spectra for the  $\text{Er}^{3+}$  complexes in DMF. Again, the shape of the spectra observed for cyc-H and cyc-D are similar, but slightly different compared to the spectrum of acyc-H.

Figure 4 shows the room temperature PL spectrum of acyc-H in KBr after excitation at 337 nm (pulse energy 20  $\mu\text{J}$ ). The 337 nm pump light is absorbed in the tail of the absorption band of the aromatic rings of the ligand. Energy transfer to the  $\text{Er}^{3+}$ -ion then leads to excitation of the  $\text{Er}^{3+}$  resulting in the observed 1.54  $\mu\text{m}$  luminescence.

Extinction spectra of the complexes in KBr are shown in Fig. 5. The absorption lines of the  $\text{Er}^{3+}$ -ion are clearly visible and are indicated in the figure (for the level notation see Fig. 1). The steadily decreasing background in the range up to 750 nm is attributed to scattering in the KBr tablets. Using measured reflection data (not shown) and taking into account the known average areal density of  $\text{Er}^{3+}$  in the samples (acyc-H  $8.54 \times 10^{18}/\text{cm}^2$ , cyc-H  $8.21 \times 10^{18}/\text{cm}^2$ , cyc-D  $9.04 \times 10^{18}/\text{cm}^2$ ), the 1.54  $\mu\text{m}$  absorption cross sections for the  $^4\text{I}_{15/2} \rightarrow ^4\text{I}_{13/2}$  transition can be derived:  $(0.62 \pm 0.05) \times 10^{-20} \text{ cm}^2$  for acyc-H,  $(1.1 \pm 0.4) \times 10^{-20} \text{ cm}^2$  for cyc-H, and  $(0.93 \pm 0.05) \times 10^{-20} \text{ cm}^2$  for cyc-D. These absorption cross sections are up to five times higher than the 1.54  $\mu\text{m}$  cross section of  $\text{Er}^{3+}$ -doped glasses,<sup>5,23</sup> and for  $\text{Er}^{3+}$ -implanted  $\text{Al}_2\text{O}_3$ .<sup>24</sup> This may be related to differences in average electron distribution around the  $\text{Er}^{3+}$ -ion for organic complexes compared to inorganic hosts.

In practice the integrated peak absorption and emission cross sections for  $\text{Er}^{3+}$  are nearly the same. Under this assumption and using the cross section derived above, the PL

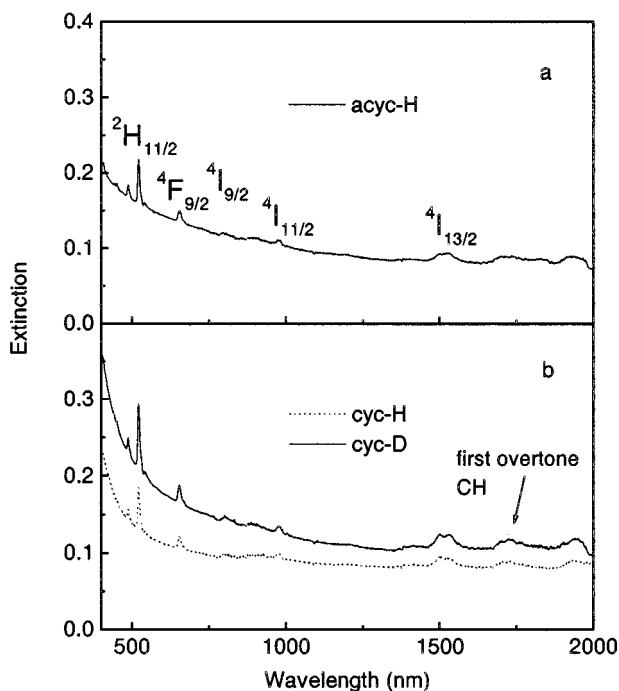


FIG. 5. Extinction spectra of the three  $\text{Er}^{3+}$ -complexes in KBr, based on transmission measurements. (a) acyc-H, (b) cyc-H and cyc-D. The absorption peaks are indicated by the level notation of the absorption band.

spectra of Fig. 3 can be converted to emission cross section spectra [see the right hand vertical scale of Fig. 3(a)]. From this spectrum the radiative lifetime  $\tau$  can be calculated:

$$\frac{1}{\tau} = \frac{8\pi n^2}{c^2} \int \nu^2 \sigma_e(\nu) d\nu, \quad (1)$$

with  $n$  the refractive index,  $c$  the speed of light, and  $\nu$  the optical frequency. Evaluating Eq. (1) yields a radiative lifetime of about 4 ms for the  $\text{Er}^{3+}$ -complexes.

The luminescence decay measurements for cyc-H in KBr and the three  $\text{Er}^{3+}$ -complexes in butanol-OD are shown in Fig. 6. Deconvolution of the laser curve from the decay curve for cyc-H in KBr results in a luminescence lifetime of

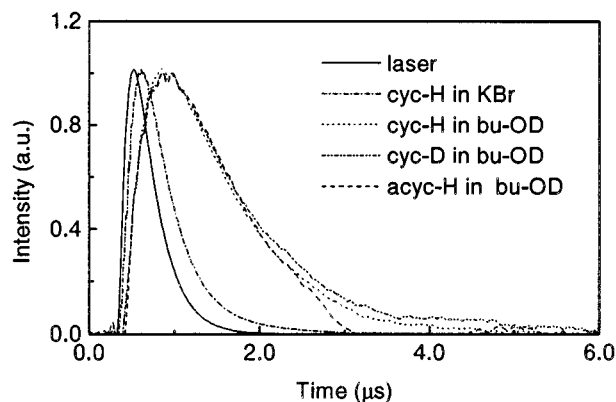


FIG. 6. Room temperature PL decay measurements for the Er-doped organic complexes in KBr and butanol-OD, excited at 337 nm at a pulse energy of 20  $\mu\text{J}$ .

TABLE I. Summary of the total Er areal density and the corresponding PL intensities for the  $\text{Er}^{3+}$ -complexes in KBr and DMF.

	Er areal density ( $\text{cm}^{-2}$ )	Relative PL intensity
acyc-H(KBr)	$8.5 \times 10^{18}$	142–193
acyc-H(DMF)	$1.3 \times 10^{18}$	113
cyc-H(KBr)	$8.2 \times 10^{18}$	210–410
cyc-H(DMF)	$1.2 \times 10^{18}$	66
cyc-D(KBr)	$9.0 \times 10^{18}$	178–242
cyc-D(DMF)	$1.2 \times 10^{18}$	66

0.5  $\mu\text{s}$ . In butanol-OD the lifetimes for the three complexes are all around 0.8  $\mu\text{s}$ . These lifetimes are much shorter than the radiative lifetime of 4 ms calculated from Eq. (1). This indicates that significant quenching of the  $\text{Er}^{3+}$  luminescence takes place.

Table I summarizes the total  $\text{Er}^{3+}$  areal density and the PL intensity for the KBr tablets and DMF solutions. For all complexes the areal density is typically a factor 7 higher in KBr than in the DMF solutions, but the luminescence intensity is only a factor 1.5–6 higher. This suggests that more luminescence quenching takes place in the KBr tablets than in the DMF solutions. A possible explanation for this difference is a concentration quenching effect: due to the mixed crystallite nature of the tablets, local concentrations of  $\text{Er}^{3+}$  may be higher than the calculated average density. Due to the local high concentration, energy transfer from one  $\text{Er}^{3+}$  ion to another can occur and the excitation can migrate among these clustered regions, followed by quenching at a defect site in the tablet. As a result the PL intensity will be lower and the luminescence lifetime shorter in the KBr tablets. In a solution where all the complexes are quite homogeneously dispersed, no concentration quenching will occur. This is confirmed by the longer luminescence lifetime for the complexes in butanol-OD solutions compared to the KBr tablets (see Fig. 6). However, even in solution the lifetimes are still much shorter than the expected 4 ms calculated from Eq. (1).

There are three possible quenching mechanisms; (1) temperature quenching, (2) quenching by the nearest C–H neighbors, (3) quenching by O–H groups.

(1) *Temperature quenching*: Figure 7 shows measurements of the integrated 1.54  $\mu\text{m}$  PL intensity between 15–300 K for the KBr tablets after direct excitation of the  $\text{Er}^{3+}$  ion at 488 nm. Cyc-H and cyc-D show the same trend as a function of temperature, with a quenching by a factor 3 between 15 K and room temperature. For acyc-H the temperature quenching is slightly smaller, a factor 2 in the same temperature range. The quenching is small and can be mainly attributed to a decrease in the absorption coefficient as the temperature is increased (resulting in less efficient excitation). This indicates that temperature quenching is not the major quenching mechanism.

(2) *Quenching by nearest C–H neighbors*: The second order vibrational energy of C–H ( $E_0 = 2960 \text{ cm}^{-1}$ ) is resonant with the  $\text{Er}^{3+}$  first excited state ( $E = 6500 \text{ cm}^{-1}$ ). This

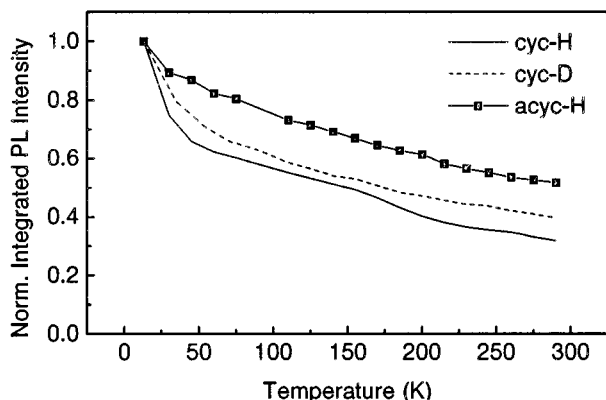


FIG. 7. Temperature dependence of the integrated  $1.54 \mu\text{m}$  PL intensity of the  $\text{Er}^{3+}$ -complexes in KBr (pump power 100 mW, excitation wavelength 488 nm).

band around  $1.7 \mu\text{m}$  can also be seen in Fig. 5. Thus, a C–H bond positioned near the  $\text{Er}^{3+}$ -ion can quench the Er luminescence. Instead, such coupling should be less for C–D ( $E_0 = 2100\text{--}2200 \text{ cm}^{-1}$ ). Comparison of the PL intensity of cyc-H with that of cyc-D for the DMF solutions (see Table I), shows that selective deuteration of the first coordination sphere has no influence on the PL intensity and thus it is concluded that quenching by these C–H bonds is not dominant.

(3) *Quenching by O–H groups:* O–H groups are present in the liquids (mainly alcohols) used in the preparation of the  $\text{Er}^{3+}$ -complexes, and they can also be present in the solvents used for the measurements: both DMF and butanol-CD are highly hygroscopic. It is therefore very likely that O–H groups are coordinated to the  $\text{Er}^{3+}$ -ion. Indeed, molecular dynamics simulations of  $\text{Ln}^{3+}$ -complexes in solution show that one O–H molecule can penetrate the first coordination shell of the ion.<sup>20</sup> In particular water may preferentially solvate the  $\text{Er}^{3+}$ -ion.<sup>25</sup> It is the most potent quencher of lanthanide luminescence, and has a significantly stronger interaction to the lanthanide than, for instance, alcohol's. An O–H group positioned near the  $\text{Er}^{3+}$ -ion will result in efficient quenching of the luminescence, because its first vibrational overtone ( $E_0 = 3400 \text{ cm}^{-1}$ ) is strongly resonant with the  $^4\text{I}_{13/2} \rightarrow ^4\text{I}_{15/2}$   $\text{Er}^{3+}$  transition ( $E = 6500 \text{ cm}^{-1}$ ). Work by Ermolaev *et al.*<sup>26</sup> shows that the rate constant for deactivation of the  $\text{Er}^{3+}$  excited state via O–H groups, located at a distance of  $2.2\text{--}2.5 \text{ \AA}$  is in the order of  $3\text{--}5 \times 10^8 \text{ s}^{-1}$ , which is dominant over deactivation via C–D bonds at  $2.2\text{--}2.5 \text{ \AA}$  ( $k = 5 \times 10^6 \text{ s}^{-1}$ ). This would explain that, with O–H attached to the complex, substitution of C–H by C–D will have no significant effect on the PL intensities measured in solution (see Table I).

#### IV. OPTICAL GAIN CALCULATION

With the coefficients determined in the previous paragraphs, an estimate of the threshold pump power for a planar optical amplifier based on Er-doped organic complexes can be made. In such a polymer channel waveguide, a high refractive index polymer [e.g., poly(phenyl methacrylate) (PPMA),  $n = 1.57$ ] doped with organic Er complexes, is em-

TABLE II. Typical values for the different parameters used for the optical gain calculation for an organic planar polymer optical amplifier.

Parameter	Symbol	Value
Erbium decay rate	$W_e$	$1.25 \times 10^6 \text{ s}^{-1}$
Erbium absorption cross section	$\sigma_e$	$1.1 \times 10^{-20} \text{ cm}^2$
Waveguide cross section	$a$	$2 \times 1 \mu\text{m}^2$
Total Er concentration	$N$	$9 \times 10^{19} \text{ cm}^{-3}$
Estimated fraction of light which is confined in the core	$\alpha$	0.4
Ligand absorption cross section	$\sigma_l$	$8.5 \times 10^{-18} \text{ cm}^2$
Ligand decay rate	$W_{lr}$	$2 \times 10^8 \text{ s}^{-1}$
Ligand nonradiative decay rate/transfer rate	$W_{lnr}$	$1 \times 10^9 \text{ s}^{-1}$

bedded in a low index polymer [e.g., poly(methyl methacrylate) (PMMA),  $n = 1.48$ ]. A typical waveguide core dimension is  $2 \times 1 \mu\text{m}^2$ .

A calculation is done for direct excitation of  $\text{Er}^{3+}$  into the  $^4\text{F}_{7/2}$  excited state (see Fig. 1). Assuming that the population of the  $^4\text{F}_{7/2}$  state decays rapidly to the first excited state, the rate equations reduce to those for a quasi-two-level system.<sup>27</sup> Solving these rate equations for “steady-state” conditions, the populations become

$$N_{ge} = \frac{W_e}{W_e + R_e}, \quad (2)$$

$$N_e = \frac{R_e}{W_e + R_e}, \quad (3)$$

where  $R_e = \sigma_e P \lambda / (hca)$  is the  $\text{Er}^{3+}$  excitation rate,  $N_e$  the population fraction of the first excited state,  $N_{ge}$  the population fraction of the ground state,  $W_e = 1/\tau_e$  the erbium decay rate,  $P$  the pump power in the waveguide,  $\sigma_e$  the absorption cross section,  $\lambda = 488 \text{ nm}$  the excitation wavelength, and  $a$  the waveguide cross section. The optical gain (dB/cm) is given by  $10 \times \log_{10}(I/I_0)$ , where  $I_0$  is the intensity at the beginning of the waveguide and  $I = I_0 e^{kx}$  along the waveguide, with  $k$  the gain factor given by

$$k = \sigma_e \{N_e - N_{ge}\} N \alpha, \quad (4)$$

with  $N$  the  $\text{Er}^{3+}$  concentration, and  $\alpha$  the estimated fraction of light which is confined in the core of the waveguide. The optical gain as a function of pump power is calculated using the values given in Table II. The result is shown in Fig. 8. The maximum gain is 1.7 dB/cm, indicating that for instance a loss free ( $1 \times 2$ ) splitter could be made with a few cm long waveguide. The threshold pump power is 930 mW. This is much higher than the minimum power needed in Er-doped glass or  $\text{Al}_2\text{O}_3$  amplifiers<sup>9</sup> and is due to the much shorter luminescence lifetime ( $0.8 \mu\text{s}$ ) of the  $\text{Er}^{3+}$  in the organic complexes as compared to that in the inorganic materials ( $> 5 \text{ ms}$ ).

The power of 930 mW needed for optical amplification is too high for any practical application. However, this problem can be solved by excitation of the complex via the aromatic part of the ligand, at 287 nm. At this wavelength the absorption cross section of the ligand is about  $8.5 \times 10^{-18} \text{ cm}^2$ , much higher than the cross section for direct absorption of the  $\text{Er}^{3+}$  ion at 488 nm ( $1\text{--}3 \times 10^{-20} \text{ cm}^2$ ).

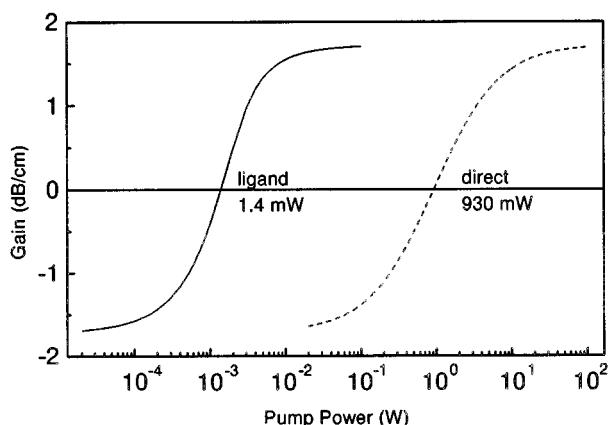


FIG. 8. Calculated optical gain as a function of pump power for direct excitation and excitation via the ligand for a waveguide amplifier with a  $2 \times 1 \mu\text{m}^2$  cross section. The threshold power is indicated for each calculation.

This makes the excitation via the ligand very efficient. Energy transfer from the ligand's excited state to the  $\text{Er}^{3+}$ -ion then results in population of the  $\text{Er}^{3+} {}^4\text{I}_{13/2}$  luminescent excited state. Taking this process into account, a new gain calculation can be made. Assuming that the transition from the singlet ( $S_1$ ) to the triplet ( $T$ ) state of the ligand is fast (see Fig. 1), a quasi-two-level system can be used for the ligand and the  $\text{Er}^{3+}$  ion. The rate equations then become

$$\frac{dN_1}{dt} = R_1 N_{\text{gl}} - W_{\text{lr}} N_1 - W_{\text{lnr}} N_1 N_{\text{ge}}, \quad (5)$$

$$\frac{dN_e}{dt} = -W_e N_e + W_{\text{lnr}} N_1 N_{\text{ge}}, \quad (6)$$

in which  $R_1 = \sigma_1 P \lambda / (hca)$  is the ligand excitation rate,  $N_e$  and  $N_1$  the population fraction of the first excited state of  $\text{Er}^{3+}$  ion and the ligand, respectively,  $N_{\text{ge}}$  and  $N_{\text{gl}}$  the population fraction in the ground state of  $\text{Er}^{3+}$ -ion and the ligand, respectively,  $W_{\text{lnr}}$  the ligand nonradiative decay rate, which couples to the  $\text{Er}^{3+}$ -ion (transfer rate),  $W_{\text{lr}}$  the ligand decay rate, including the nonradiative decay which is not coupled to the  $\text{Er}^{3+}$ -ion, and  $\sigma_1$  the ligand absorption cross section.

Solving these equations for steady-state conditions, the gain can be calculated using Eq. (4) and typical values given in Table II. The result is also plotted in Fig. 8. The threshold pump power reduces from 930 to 1.4 mW. These low pump powers are very interesting for practical applications. Note that in the final design pump loss has to be taken into account. The next challenge is to engineer the ligand and to shift the excitation wavelength to the visible in order to be able to use standard semiconductor lasers as pump lasers. Alternatively, sensitizers with a high absorption coefficient and a high intersystem crossing efficiency, may be attached to the complex, to further optimize the pump efficiency. This work is going on at present. Finally we note that the above calculations do not take into account upconversion effects, which may increase the pump power needed for amplification.<sup>28</sup> More measurements are required to determine

the cooperative upconversion and excited state absorption cross sections for these  $\text{Er}^{3+}$ -doped organic complexes.

## V. CONCLUSIONS

Erbium-doped polydentate hemispherand organic cage complexes show a broad (70 nm FWHM) photoluminescence spectrum at room temperature centred around 1.54  $\mu\text{m}$ . The  $\text{Er}^{3+}$ -ion can be excited directly in the  $4f$  manifold, or indirectly via the aromatic rings of the complex. When dissolved in butanol-OD the luminescence lifetime is 0.8  $\mu\text{s}$ , much shorter than the estimated radiative lifetime of 4 ms. This is attributed to the presence of O–H groups, present in molecules located in the first coordination shell of the complex, which serve as quenching sites for the excited  $\text{Er}^{3+}$ -ion. The O–H most likely originates from the water which is present during the chemical synthesis or in the solution in which the complexes are dissolved. Optical gain calculations show that these  $\text{Er}^{3+}$ -doped organic complexes, when dissolved in a polymer channel waveguide, may show net optical amplification for a pump power as low as 1.4 mW and with a typical gain of 1.7 dB/cm.

## ACKNOWLEDGMENTS

This work is part of the research program of the foundation for Fundamental Research on Matter and was made possible by financial support from NWO, STW, and the IOP Electro-optics Program. Frank A. J. Geurts (Akzo Nobel Central Research) is greatly acknowledged for doing the time resolved measurements and the optical absorption measurements.

- <sup>1</sup>E. Desurvire, *Sci. Am. (Int. Ed.)* **266**, 96 (1992).
- <sup>2</sup>A. M. Glass, *Phys. Today* **46**, 34 (1993).
- <sup>3</sup>E. Desurvire, *Phys. Today* **47**, 20 (1994).
- <sup>4</sup>W. J. Miniscalco, *J. Lightwave Technol.* **9**, 234 (1991).
- <sup>5</sup>E. Snoeks, G. N. van den Hoven, and A. Polman, *J. Appl. Phys.* **73**, 8179 (1993).
- <sup>6</sup>G. N. van den Hoven, E. Snoeks, A. Polman, J. M. W. van Uffelen, Y. S. Oei, and M. K. Smit, *Appl. Phys. Lett.* **62**, 3065 (1993).
- <sup>7</sup>T. Feuchter, E. K. Mwarania, J. Wang, L. Reekie, and J. S. Williams, *IEEE Photonics Technol. Lett.* **4**, 542 (1991).
- <sup>8</sup>T. Kitagawa, K. Kitagawa Hattori, K. Shuto, M. Yasu, M. Kobayashi, and M. Horiguchi, *Electron. Lett.* **28**, 1818 (1992).
- <sup>9</sup>G. Nykolak, M. Haner, P. C. Becker, J. Schmulovich, and Y. H. Wong, *IEEE Photonics Technol. Lett.* **5**, (1993).
- <sup>10</sup>K. Hattori, T. Kitagawa, M. Oguma, Y. Ohmori, and M. Horiguchi, *Electron. Lett.* **30**, 856 (1994).
- <sup>11</sup>D. Barbier, P. Gastaldo, B. Hyde, J. M. Jouanno, and A. Kevorkian, in *Proceedings of the 7th European Conference on Integrated Optics* (Delft University of Technology, Delft, 1995), p. 241.
- <sup>12</sup>M. Hempstead, J. E. Román, C. C. Ye, J. S. Wilkinson, P. Camy, P. Laborde, and C. Lermieux, in *Proceedings of the 7th European Conference on Integrated Optics* (Delft University of Technology, Delft, 1995), p. 233.
- <sup>13</sup>G. N. van den Hoven, R. J. I. M. Koper, A. Polman, C. van Dam, J. W. M. van Uffelen, and M. K. Smit, *Appl. Phys. Lett.* **68**, 1886 (1996).
- <sup>14</sup>P. Becker, R. Brinkmann, M. Dinand, W. Sohler, and H. Suche, *Appl. Phys. Lett.* **61**, 1257 (1992).
- <sup>15</sup>R. Brinkmann, I. Baumann, M. Dinand, W. Sohler, and H. Suche, *IEEE J. Quantum Electron.* **30**, 2356 (1994).
- <sup>16</sup>B. Booth, *Polymers for Lightwave and Integrated Optics*, edited by L. A. Hornak (Dekker, New York, 1992).
- <sup>17</sup>V. P. Gapontsev, A. A. Izyneev, Yu. E. Sverchov, and M. R. Syrtlanov, *Sov. J. Quantum Electron.* **11**, 1101 (1981).
- <sup>18</sup>A. J. Bruce, W. A. Reed, A. E. Neeves, L. R. Copeland, W. H.

- Grodziewicz, and A. Lidgard, *Mater. Res. Soc. Symp. Proc.* **244**, 157 (1992).
- <sup>19</sup>Y. Yan, A. J. Faber, and H. de Waal, *J. Non-Cryst. Solids* **181**, 283 (1995).
- <sup>20</sup>M. P. Oude Wolbers, F. C. J. M. van Veggel, B. H. M. Snellink-Ruël, J. W. Hofstraat, F. A. J. Geurts, and D. N. Reinhoudt, *J. Am. Chem. Soc.* **119**, 138 (1997).
- <sup>21</sup>A. Polman, D. C. Jacobson, D. J. Eaglesham, R. C. Kistler, and J. M. Poate, *J. Appl. Phys.* **70**, 3778 (1991).
- <sup>22</sup>W. J. Miniscalco, *J. Lightwave Technol.* **9**, 234 (1991).
- <sup>23</sup>J. N. Sandoe, P. H. Sarkies, and S. Parke, *J. Phys. D* **5**, 1788 (1972).
- <sup>24</sup>G. N. van den Hoven, E. Snoeks, J. A. van der Elsken, C. van Dam, J. M. W. van Uffelen, and M. K. Smit, *Appl. Opt.* **36**, 3338 (1997).
- <sup>25</sup>M. P. Oude Wolbers, thesis, University of Twente, 1997.
- <sup>26</sup>V. L. Ermolaev and E. B. Sveshnikova, *Russ. Chem. Rev.* **63**, 905 (1994).
- <sup>27</sup>C. K. Jørgensen, *Lasers and Excited States of Rare Earths* (Springer, New York, 1977).
- <sup>28</sup>G. N. van den Hoven, E. Snoeks, A. Polman, C. van Dam, J. M. W. van Uffelen, and M. K. Smit, *J. Appl. Phys.* **79**, 1258 (1996).